ChemComm

COMMUNICATION

View Article Online
View Journal | View Issue

Cite this: *Chem. Commun.*, 2015, 51, 11773

Received 20th April 2015,
Accepted 8th June 2015

DOI: 10.1039/c5cc03267a

www.rsc.org/chemcomm

Ion-precursor and ion-dose dependent anti-galvanic reduction†

Shubo Tian,‡ Chuanhao Yao,‡ Lingwen Liao, Nan Xia and Zhikun Wu*

Controlling alloy nanoparticles with atomic monodispersity is challenging, and the recently revealed anti-galvanic reduction (AGR) provides a unique solution to this challenge. Herein we demonstrate that AGR is ion-precursor and ion-dose dependent, which offers novel strategies to tune the composition, structure and properties of nanoparticles by varying the ion-precursor and ion-dose in the AGR reaction.

Bimetal nanoparticles have attracted extensive interest for many years due to their intriguing properties, which are not exhibited by mono-metal nanoparticles.[1–6] To insightfully understand the properties of bimetal nanoparticles, controlling bimetal nanoparticles with atomic monodispersity is of prime importance. Enormous effort has been put into the achievement of this aim.[4,7–15] A popular method for the synthesis of atomically precise bimetal nanoparticles is the synchro-synthesis method which was once utilized for the synthesis of $Au_{24}Pd(SR)_{18}$ (SR = $SC_{12}H_{25}$, SC_2H_4Ph, $S(CH_2CH_2O)_5CH_3$),[16,17] $Au_{24}Pt(SR)_{18}$ (SR = SC_2H_4Ph),[18] $Au_{25-x}Cu_x$ $(SR)_{18}$ (SR = SeC_8H_{17}),[19] $Au_{25-x}Ag_x(SR)_{18}$ (SR = $SC_{12}H_{25}$, SC_2H_4Ph, $SC_nH_{2n}COOH$),[8,13,20,21] $Au_{38-x}Ag_x(SR)_{18}$ (SR = SC_2H_4Ph),[22] $Au_{36}Pd_2(SR)_{24}$ (SR = SC_2H_4Ph),[23] *etc.* However, only a few bimetal nanoparticles with atomic monodispersity were obtained by this method;[16–18] galvanic reduction (GR) is another well-known method for engineering the composition, structure and properties of nanoparticles.[7,24–35] Unfortunately, no atomically monodisperse bimetal nanoparticles (AMBN) have been reported so far using GR. Overall, the synthesis of AMBN is still challenging. Fortunately, the recently revealed anti-galvanic reduction (AGR) provides a unique strategy to access AMBN[36–42] and very recently atomically mono-disperse $Au_{25}Ag_2(PET)_{18}$ (PET = SC_2H_4Ph)[42] was successfully synthesized in two minutes, in high yield (89%) and on a gram scale by this unusual method. Interestingly, it is shown that when the silver ion is replaced by Cu^{2+} in the reaction with the anion $Au_{25}(PET)_{18}$, $Au_{44}(PET)_{32}$[41] instead of the Au/Cu bimetal nanoparticles can be obtained, which indicates that AGR is dependent on the ion species and not only limited to the synthesis of alloy nanoparticles. One possible reason is that different ion species possess various reduction potentials and coordination natures. A question naturally arising is whether AGR is dependent on the ion precursors which influence the ion (or its reduction state) release. To unravel this question, we tested the reaction between the anion $Au_{25}(PET)_{18}^-$ ($N(C_8H_{17})_4^+$ as the counter ion) and four different silver ion precursors. Indeed, the experimental results demonstrate that AGR is ion-precursor dependent, and additional experiments reveal that AGR is also ion-dose dependent. Below we present more details and discussion.

EDTA, DTZ and PET are some common chelates for metal ions, and they exhibit different chelating natures and abilities towards silver ions/atoms (*i.e.* Ag–EDTA, Ag–PET and Ag–DTZ complexes have distinctly different releasing abilities of silver ions/atoms), so Ag–EDTA, Ag–PET and Ag–DTZ complexes plus $AgNO_3$ were chosen as silver ion precursors due to their exhibition of various releasing abilities of silver ions/atoms (EDTA: ethylenediamine tetraacetic acid disodium salt; PET: 2-phenylethanethiol; DTZ: dithizone). First, the Ag–EDTA, Ag–PET and Ag–DTZ complexes were prepared by simply mixing the according ligand with $AgNO_3$, then they together with $AgNO_3$ were added into a toluene solution of the anion $Au_{25}(PET)_{18}$ (for convenience of comparison, the $Ag/Au_{25}(PET)_{18}$ molar ratio in all cases was 2 : 1). One hour later, the four reactions were stopped by the addition of excessive petroleum ether, the as-obtained precipitates were collected and thoroughly washed with methanol, then used for thin-layer chromatography (TLC) analyses[42,43] (CH_2Cl_2–petroleum ether as developing solvent). It should be noted that the whole process (including reaction, post-treatment and analysis by TLC) was facilely conducted at room temperature without the avoidance of light and air. Interestingly, TLC results show a distinct difference

Key Laboratory of Materials Physics, Anhui Key Laboratory of Nanomaterials and Nanostructures, Institute of Solid State Physics, Chinese Academy of Sciences, Hefei 230031, China. E-mail: zkwu@issp.ac.cn

† Electronic supplementary information (ESI) available: Detailed information about the synthesis, characterizations and MALDI-TOF-MS spectra of S6, S7 and S9. See DOI: 10.1039/c5cc03267a

‡ S.T. and C.Y. contributed equally to this work.

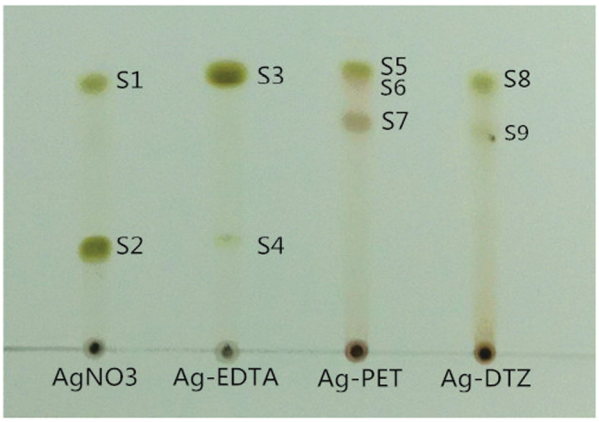

Fig. 1 Photograph of the TLC plate. From left to right, AgNO3, Ag–EDTA, Ag–PET and Ag–DTZ were used as the precursor.

between the product components in the four cases (see Fig. 1, from left to right, $AgNO_3$, Ag–EDTA, Ag–PET and Ag–DTZ were used as the silver ion precursor). For convenience, the spots in the TLC plate were sequentially numbered as S1–S9 (see Fig. 1). It is clear that the products contain a minor component S1 and a major component S2 when $AgNO_3$ was used as the silver-ion resource; when Ag–EDTA was used as the silver ion precursor, the products contain a dominant component S3 and a trace of component S4; in the case of Ag–PET, the products are a little complex and there are two comparable components, S5 and S7, together with one minor component S6; in the case of Ag–DTZ, one distinct component S8 and a trace of component S9 were found in the TLC plate. Preliminarily judged by the TLC results, S3 and S5 may be the same compound since they show the same mobility and colour in the plate. Similarly, S2 and S4 may be identical. To identify the components, all of them (S1–S9) were isolated from a preparative thin-layer chromatography (PTLC) plate and further analyzed using UV/Vis/NIR spectrometry, together with matrix-assisted laser desorption/ionization time of flight mass spectrometry (MALDI-TOF-MS). UV/Vis/NIR spectra reveal that both S3 and S5 are neutral $Au_{25}(PET)_{18}$[44,45] (see Fig. 2), which was further confirmed using MALDI-TOF-MS (see Fig. 3). UV/Vis/NIR spectra, together with MALDI-TOF-MS reveal that S2 and S4 are indeed identical $Au_{25}Ag_2(PET)_{18}$, alloy nanoparticles which we reported very recently.[42] Surprisingly, S1 is identified to be a mixture of $Au_{25}(PET)_{18}$ (major) and $Au_{24}Ag(PET)_{18}$ (minor) by MALDI-TOF-MS (Fig. 3), and S8 concurrently contains $Au_{25}(PET)_{18}$ (minor), $Au_{24}Ag(PET)_{18}$ (major) and $Au_{23}Ag_2(PET)_{18}$ (minor), which indicate that MALDI-TOF-MS is a better way to monitor the purity of such samples than TLC and UV/Vis/NIR spectroscopy. Unfortunately, the fragmentation in MALDI-TOF-MS retards the rational assignments of S6, S7 and S9 (Fig. S1–S3, ESI†), and further efforts are underway to grow high quality single crystals and they are hereafter not discussed in this work. A summary of the assignments of the TLC spots is shown in Table 1, which clearly demonstrates that AGR is strongly dependent on the ion-precursor. Interestingly, the starting spots also show a difference between the anion $Au_{25}(PET)_{18}$ and ion precursors demonstrated by UV/Vis/NIR and

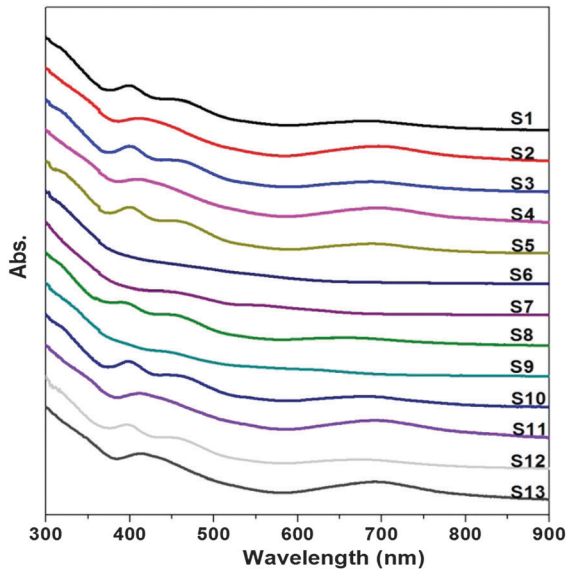

Fig. 2 UV/Vis/NIR spectra of S1–S13.

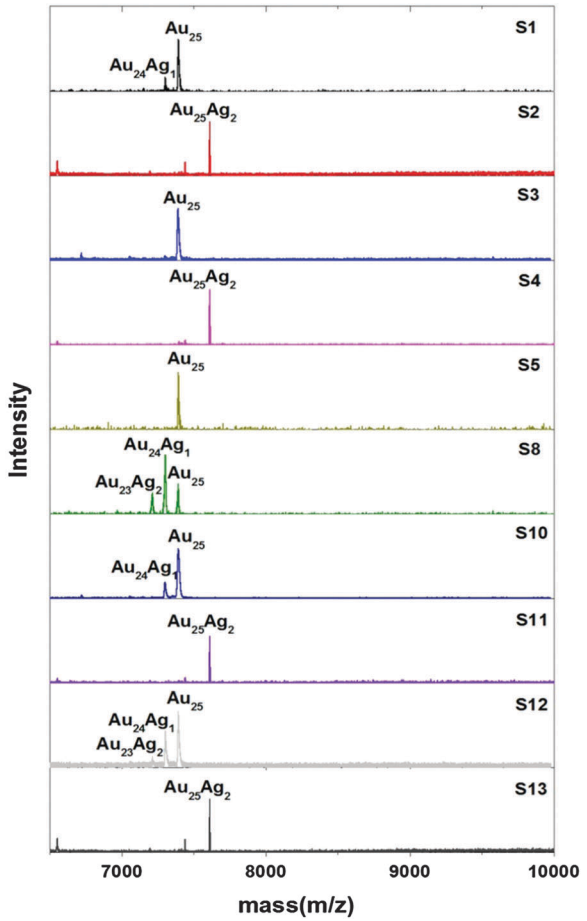

Fig. 3 MALDI-TOF-MS spectra of S1–S5, S8 and S10–S13. The mass spectra of S1, S3, S5, S8, S10, S12 were acquired in the negative ionization mode, while the remaining spectra were recorded in the positive ionization mode.

Table 1 Summary of the assignments of TLC spots

Precursor	2 eq. $AgNO_3$	2 eq. Ag–EDTA	2 eq. Ag–PET	2 eq. Ag–DTZ	0.5 eq. Ag–DTZ	1 eq. Ag–DTZ
	$Au_{25-x}Ag_x(PET)^0_{18}$, (S1; x = 0, 1) $Au_{25}Ag_2(PET)^0_{18}$, (S2)	$Au_{25}(PET)^0_{18}$, (S3) $Au_{25}Ag_2(PET)^0_{18}$, (S4)	$Au_{25}(PET)^0_{18}$, (S5) Unknown (S6, S7)	$Au_{25-x}Ag_x(PET)^0_{18}$, (S8; x = 0, 1, 2) Unknown (S9)	$Au_{25-x}Ag_x(PET)^0_{18}$, (S10; x = 0, 1) $Au_{25}Ag_2(PET)^0_{18}$, (S11)	$Au_{25-x}Ag_x(PET)^0_{18}$, (S12; x = 0, 1, 2) $Au_{25}Ag_2(PET)^0_{18}$, (S13)

MALDI-TOF-MS (Fig. S4–S8, ESI†): peaks centered at m/z ~11 K and ~8.9 K in the mass spectra (Fig. S5 and S7, ESI†) indicate the formation of some big nanoclusters (compared with $Au_{25}(PET)_{18}$) when $AgNO_3$ and Ag–PET were employed as the ion precursors, the m/z ~6030 peak in Fig. S6 (ESI†) indicates the production of small immobile nanoclusters when Ag–EDTA was used as the ion precursor, while the absence of peaks in the m/z range from 2000 to 20 000 in Fig. S8 (ESI†), together with the absence of a plasma peak (~520 nm) in Fig. S4 (ESI†) and the detection of Au using XPS (Fig. S9 and S10, ESI†) indicates that $Au_{25}(PET)_{18}$ partially decomposes to very small nanoclusters or complexes in the case of Ag–DTZ. These results further demonstrate that AGR is ion-precursor dependent. As proposed above, the ion (ion reduced state) release ability of the ion precursor may partly contribute to the ion-precursor dependence of AGR since the main product is $Au_{25}Ag_2(PET)_{18}$ when $AgNO_3$ was used as the ion precursor, while in the other three cases $Au_{25}Ag_2(PET)_{18}$ is a minor product or even not found. Another consideration for the ion-precursor dependence is that the ligand may assist the atom replacement or recombination in AGR, which can be deduced from the fact that S8 mainly contains $Au_{24}Ag(PET)_{18}$ (Ag–DTZ as the precursor) while S1 mainly contains neutral Au_{25} accompanied by a minor amount of $Au_{24}Ag(PET)_{18}$ ($AgNO_3$ as the ion precursor).

The dominance of $Au_{24}Ag(PET)_{18}$ in S8 gives rise to a question: which is preferential in AGR, the simple oxidation of $Au_{25}(PET)_{18}$ (from the anion $Au_{25}(PET)_{18}$ to neutral $Au_{25}(PET)_{18}$) or the replacement of gold by silver (formation of $Au_{25-x}Ag_x(PET)_{18}$)? It is clear that the former is preferential in the case when $AgNO_3$ was used as the ion-precursor, however, it looks like the reverse in the case of Ag–DTZ (but a possible reason is the excess of the silver precursor). To clarify this, we decreased the Ag/$Au_{25}(PET)_{18}$ molar ratio to 1 : 1 and 1 : 0.5, and additionally tested two reactions between the anion $Au_{25}(PET)_{18}$[46] and Ag–DTZ. It is revealed by MALDI-TOF-MS that in the case of a low dose of Ag–DTZ the dominant component of S10 and S12 (Fig. 3 and 4) is neutral $Au_{25}(PET)_{18}$ (in strong contrast to the case of S8, see Fig. 1–4), and with the increase of the Ag–DTZ dose the mono-replacement alloy nanoparticles ($Au_{24}Ag(PET)_{18}$) increase and even the bi-replacement nanoparticles ($Au_{23}Ag_2(PET)_{18}$) appear. The experimental results clearly show that the simple oxidation is preferential to the replacement in the reaction between the anion $Au_{25}(PET)_{18}$ and Ag–DTZ too. Another interesting finding is the concurrent formation of $Au_{25}Ag_2(PET)_{18}$ identified using TLC, UV/Vis/NIR spectrometry and MALDI-TOF-MS in the case of low doses of Ag–DTZ (see Fig. 2 and 3). Taken together, these facts demonstrate that the AGR is also dose-dependent: the dose of Ag–DTZ can influence not only the relative content of neutral $Au_{25}(PET)_{18}$ and doped $Au_{25}(PET)_{18}$,

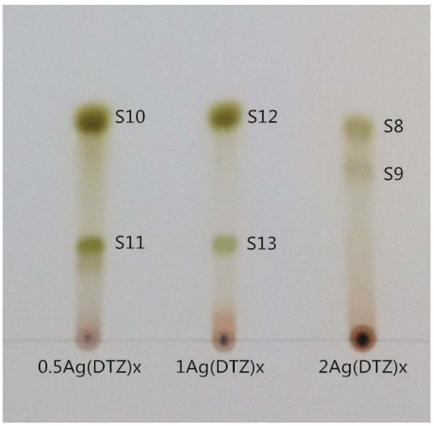

Fig. 4 Photograph of the TLC plate. From left to right; 0.5 eq., 1 eq. and 2 eq. Ag–DTZ were used in the AGR reaction.

but also the product types. It's expected that novel nanoparticles (including alloy nanoparticles) can be synthesized by varying the ion-precursor and ion-dose in the AGR reaction, thus the advancement of AGR research in this work provides enormous and unusual opportunities for tuning the composition, structure and properties of nanoparticles.

In summary, in this work we demonstrate that AGR is ion-precursor and ion-dose dependent, and we also reveal that the simple oxidation of the anion $Au_{25}(PET)_{18}$ is preferential for the concurrent replacement of gold in $Au_{25}(PET)_{18}$ by silver in cases of a low dose of silver ion-precursor. The significance and novelty of this work lie in: it provides novel mechanistic insight into AGR, and paves a way to tune the composition, structure and properties of nanoparticles by varying the ion precursor and ion dose in AGR reactions.

This work was supported by the National Basic Research Program of China (Grant No. 2013CB934302), the Natural Science Foundation of China (No. 21222301, 21171170), the Ministry of Human Resources and Social Security of China, the Innovative Program of Development Foundation of Hefei Center for Physical Science and Technology (2014FXCX002), the CAS/SAFEA International Partnership Program for Creative Research Teams and the ''Hundred Talents Program'' of the Chinese Academy of Sciences.

Notes and references

1 V. R. Stamenkovic, B. Fowler, B. S. Mun, G. Wang, P. N. Ross, C. A. Lucas and N. M. Markovic, *Science*, 2007, **315**, 493–497.
2 B. Lim, M. Jiang, P. H. C. Camargo, E. C. Cho, J. Tao, X. Lu, Y. Zhu and Y. Xia, *Science*, 2009, **324**, 1302–1305.
3 R. Subbaraman, D. Tripkovic, D. Strmcnik, K.-C. Chang, M. Uchimura, A. P. Paulikas, V. Stamenkovic and N. M. Markovic, *Science*, 2011, **334**, 1256–1260.

4 H. Yang, Y. Wang, H. Huang, L. Gell, L. Lehtovaara, S. Malola, H. Hakkinen and N. Zheng, *Nat. Commun.*, 2013, **4**, 2422.
5 C. Chen, Y. Kang, Z. Huo, Z. Zhu, W. Huang, H. L. Xin, J. D. Snyder, D. Li, J. A. Herron, M. Mavrikakis, M. Chi, K. L. More, Y. Li, N. M. Markovic, G. A. Somorjai, P. Yang and V. R. Stamenkovic, *Science*, 2014, **343**, 1339–1343.
6 G. Chen, Y. Zhao, G. Fu, P. N. Duchesne, L. Gu, Y. Zheng, X. Weng, M. Chen, P. Zhang, C.-W. Pao, J.-F. Lee and N. Zheng, *Science*, 2014, **344**, 495–499.
7 Y.-S. Shon, G. B. Dawson, M. Porter and R. W. Murray, *Langmuir*, 2002, **18**, 3880–3885.
8 Y. Negishi, T. Iwai and M. Ide, *Chem. Commun.*, 2010, **46**, 4713–4715.
9 Y. Negishi, K. Munakata, W. Ohgake and K. Nobusada, *J. Phys. Chem. Lett.*, 2012, **3**, 2209–2214.
10 T. Udayabhaskararao, Y. Sun, N. Goswami, S. K. Pal, K. Balasubramanian and T. Pradeep, *Angew. Chem., Int. Ed.*, 2012, **51**, 2155–2159.
11 H. Yang, Y. Wang, J. Lei, L. Shi, X. Wu, V. Maekinen, S. Lin, Z. Tang, J. He, H. Haekkinen, L. Zheng and N. Zheng, *J. Am. Chem. Soc.*, 2013, **135**, 9568–9571.
12 N. Barrabes, B. Zhang and T. Buergi, *J. Am. Chem. Soc.*, 2014, **136**, 14361–14364.
13 C. Kumara, C. M. Aikens and A. Dass, *J. Phys. Chem. Lett.*, 2014, **5**, 461–466.
14 S. Wang, X. Meng, A. Das, T. Li, Y. Song, T. Cao, X. Zhu, M. Zhu and R. Jin, *Angew. Chem., Int. Ed.*, 2014, **53**, 2376–2380.
15 H. Yang, Y. Wang, J. Yan, X. Chen, X. Zhang, H. Hakkinen and N. Zheng, *J. Am. Chem. Soc.*, 2014, **136**, 7197–7200.
16 C. A. Fields-Zinna, M. C. Crowe, A. Dass, J. E. F. Weaver and R. W. Murray, *Langmuir*, 2009, **25**, 7704–7710.
17 Y. Negishi, W. Kurashige, Y. Niihori, T. Iwasa and K. Nobusada, *Phys. Chem. Chem. Phys.*, 2010, **12**, 6219–6225.
18 H. Qian, D.-e. Jiang, G. Li, C. Gayathri, A. Das, R. R. Gil and R. Jin, *J. Am. Chem. Soc.*, 2012, **134**, 16159–16162.
19 W. Kurashige, K. Munakata, K. Nobusada and Y. Negishi, *Chem. Commun.*, 2013, **49**, 5447–5449.
20 D. R. Kauffman, D. Alfonso, C. Matranga, H. Qian and R. Jin, *J. Phys. Chem. C*, 2013, **117**, 7914–7923.
21 X. Y. Dou, X. Yuan, Q. F. Yao, Z. T. Luo, K. Y. Zheng and J. P. Xie, *Chem. Commun.*, 2014, **50**, 7459–7462.
22 C. Kumara and A. Dass, *Nanoscale*, 2012, **4**, 4084–4086.
23 Y. Negishi, K. Igarashi, K. Munakata, W. Ohgake and K. Nobusada, *Chem. Commun.*, 2012, **48**, 660–662.
24 L. A. Porter, A. E. Ribbe and J. M. Buriak, *Nano Lett.*, 2003, **3**, 1043–1047.
25 J. Y. Chen, B. Wiley, J. McLellan, Y. J. Xiong, Z. Y. Li and Y. N. Xia, *Nano Lett.*, 2005, **5**, 2058–2062.
26 S. E. Skrabalak, L. Au, X. Li and Y. Xia, *Nat. Protoc.*, 2007, **2**, 2182–2190.
27 L. Au, X. Lu and Y. Xia, *Adv. Mater.*, 2008, **20**, 2517–2522.
28 Q. B. Zhang, J. P. Xie, J. Y. Lee, J. X. Zhang and C. Boothroyd, *Small*, 2008, **4**, 1067–1071.
29 M. Rycenga, C. M. Cobley, J. Zeng, W. Li, C. H. Moran, Q. Zhang, D. Qin and Y. Xia, *Chem. Rev.*, 2011, **111**, 3669–3712.
30 Y. Xia, W. Li, C. M. Cobley, J. Chen, X. Xia, Q. Zhang, M. Yang, E. C. Cho and P. K. Brown, *Acc. Chem. Res.*, 2011, **44**, 914–924.
31 K. W. Kim, S. M. Kim, S. Choi, J. Kim and I. S. Lee, *ACS Nano*, 2012, **6**, 5122–5129.
32 W. Zhang, J. Yang and X. Lu, *ACS Nano*, 2012, **6**, 7397–7405.
33 C. Zhu, S. Guo and S. Dong, *Adv. Mater.*, 2012, **24**, 2326–2331.
34 M. Liu, Y. Lu and W. Chen, *Adv. Funct. Mater.*, 2013, **23**, 1289–1296.
35 C. Wang, Y. Wang, L. Xu, X. Shi, X. Li, X. Xu, H. Sun, B. Yang and Q. Lin, *Small*, 2013, **9**, 413–420.
36 Z. Wu, *Angew. Chem., Int. Ed.*, 2012, **51**, 2934–2938.
37 X. W. Liu, D. S. Wang and Y. D. Li, *Nano Today*, 2012, **7**, 448–466.
38 G. L. Liu, D. Q. Feng, W. J. Zheng, T. F. Chen and D. Li, *Chem. Commun.*, 2013, **49**, 7941–7943.
39 J. Sun, H. X. Wu and Y. D. Jin, *Nanoscale*, 2014, **6**, 5449–5457.
40 M. Wang, Z. Wu, Z. Chu, J. Yang and C. Yao, *Chem. – Asian J.*, 2014, **9**, 1006–1010.
41 M. B. Li, S. K. Tian, Z. Wu and R. Jin, *Chem. Commun.*, 2015, **51**, 4433–4436.
42 C. Yao, J. Chen, M.-B. Li, L. Liu, J. Yang and Z. Wu, *Nano Lett.*, 2015, **15**, 1281–1287.
43 A. Ghosh, J. Hassinen, P. Pulkkinen, H. Tenhu, R. H. Ras and T. Pradeep, *Anal. Chem.*, 2014, **86**, 12185–12190.
44 M. Z. Zhu, W. T. Eckenhoff, T. Pintauer and R. C. Jin, *J. Phys. Chem. C*, 2008, **112**, 14221–14224.
45 Z. Wu and R. Jin, *Nano Lett.*, 2010, **10**, 2568–2573.
46 Z. Wu, J. Suhan and R. Jin, *J. Mater. Chem.*, 2009, **19**, 622–626.

